Science of the Total Environment 557–558 (2016) 395–403

Contents lists available at ScienceDirect

Science of the Total Environment

journal homepage: www.elsevier.com/locate/scitotenv

The concentration-dependent aggregation of Ag NPs induced by cystine

K. Afshinnia, I. Gibson, R. Merrifield, M. Baalousha *

Center for Environmental Nanoscience and Risk, Department of Environmental Health Sciences, Arnold School of Public Health, University South Carolina, Columbia, SC 29208, United States

HIGHLIGHTS

- Effect of cystine on the aggregation of AgNPs was investigated
- UV-vis was used to monitor the aggregation behavior of Ag NPs
- Cystine caused aggregation of charge and sterically stabilized AgNPs
- The critical coagulation concentration decreased at lower AgNP concentrations
- The impact of cysteine/cystine on Ag NP behavior in biological/toxicological media should be carefully evaluated

GRAPHICAL ABSTRACT

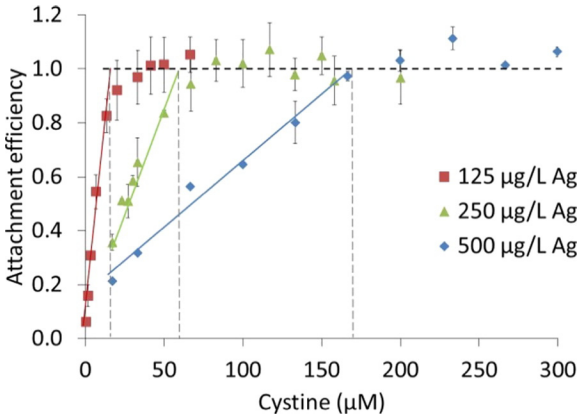

ARTICLE INFO

Article history:
Received 23 December 2015
Received in revised form 25 February 2016
Accepted 26 February 2016
Available online xxxx

Editor: Kevin V. Thomas

Keywords:
AgNPs
Cystine
Aggregation kinetics
UV–vis

ABSTRACT

Cystine is widely used in cell culture media. Cysteine, the reduced form of cystine, is widely used to scavenge dissolved Ag in eco-toxicological studies to differentiate dissolved vs. nanoparticle uptake and toxicity. However, little is known about the impact of cysteine and cystine on the aggregation behavior of Ag NPs, in particular as a function of Ag NP concentration. Herein, we investigate how cystine (0–300 μM) affects the stability of citrate-, polyvinylpyrrolidone-, and polyethylene glycol-coated silver nanoparticles (cit-Ag NPs, PVP-Ag NPs and PEG-Ag NPs, respectively) with and without Suwannee River fulvic acid (SRFA) as a function of Ag NPs concentration using UV–vis spectroscopy at environmentally and ecotoxicologically relevant Ag NP concentrations (ca. 125–1000 μg L^{-1}). The results demonstrate, for the first time, the concentration-dependent aggregation of cit-Ag NPs in the presence of cystine with a shift in the critical coagulation concentration (CCC) to lower cystine concentrations at lower cit-Ag NP concentrations. At the highest cit-Ag NP concentration (1000 μg L^{-1}), reaction limited aggregation was only observed and no CCC was measured. SRFA slowed the aggregation of cit-Ag NPs by cystine and aggregation occurred in reaction limited aggregation (RLA) regime only. No CCC value was measured in the presence of SRFA. Cystine replaces citrate, PVP and PEG coatings, resulting in aggregation of both electrostatically and sterically stabilized Ag NPs. These findings are important in understanding the factors determining the behavior of Ag NPs in cell culture media. Also due to the similarity between cystine and cysteine, these results are important in understanding the uptake and toxicity of Ag NPs vs. Ag ions, and suggest that the reduction of the toxicity of Ag NPs in the presence of cysteine could be due to a combined effect of scavenging Ag^{+} ions and Ag NP aggregation in the presence of cysteine.

* Corresponding author.
E-mail address: mbaalous@mailbox.sc.edu (M. Baalousha).

http://dx.doi.org/10.1016/j.scitotenv.2016.02.212
0048-9697/

1. Introduction

The rapid development of nanotechnology and concern regarding the potential environmental and human health implication of nanoparticles (NPs) has spurred extensive interest in understanding the behavior, fate and effects of NPs (NNI, 2014; Royal Society and Royal Academy Engineering Nanoscience and Nanotechnologies, 2004; Mirshahghassemi and Lead, 2015). Silver NPs (Ag NPs) are among the most widely used NPs in consumer products as antimicrobial agent (Woodrow Wilson data base, 2014). Several studies have suggested that Ag NPs can be released from nano-enabled products and find their way to the environment, resulting in environmental and human exposure to Ag NPs (Benn and Westerhoff, 2008; Kaegi et al., 2010).

Considerable research has been conducted to better understand the effect of Ag NPs on a wide range of organisms and cell lines (Sharma et al., 2014), with a particular attention given to differentiate the NP from dissolved metal effects due to the known solubility of Ag NPs (Navarro et al., 2008; Smetana et al., 2008; Lubick, 2008; Miao et al., 2011). Several studies have reported mixed results; some show particle-specific toxicity (Navarro et al., 2008; Silva et al., 2014; El Badawy et al., 2011; George et al., 2012), others predominantly relate the effect to free Ag^+ ions (Xiu et al., 2012; Jin et al., 2010), while other studies suggested combined effect of Ag NPs and free Ag^+ ions (Pokhrel et al., 2014; Kawata et al., 2009). These controversies could be partially due to the lack of understanding of NP behavior in the ecotoxicological media (Sharma et al., 2014), in particular at ecotoxicologically relevant concentrations (Baalousha, 2009; Baalousha et al., 2015a).

To differentiate Ag^+ from Ag NPs effect, binding ligands (e.g. Cl^- and cysteine) are typically used to complex the released silver ions from Ag NPs (Navarro et al., 2008; Kawata et al., 2009), with little understanding of the impact of the ligands (e.g. cysteine) on the behavior of Ag NPs in the test medium. Several studies have reported reduced toxicity of Ag NP suspension in the presence of cysteine and attributed this reduction solely to the complexation of free Ag^+ ions by cysteine (Navarro et al., 2008; Kawata et al., 2009), without considering the potential destabilization of Ag NPs in the presence of cysteine. Therefore, understanding the interaction between Ag NPs and cysteine is an important issue to underpin the assessment of dissolved silver and Ag NP uptake and toxicity in aquatic organisms. Additionally cystine, the oxidized form of cysteine, is widely used in cell culture media (http://www.sigmaaldrich.com/life-science/cell-culture/learning-center/media-expert/cysteine.html). Cysteine and cystine are essential amino acids in cell culture media that must be supplied from an exogenous source.

On the other hand, the fate, transport and effects of Ag NPs in the environment depends on their interaction with naturally ubiquitous organic ligands such as thiols (cysteine), disulfide (cystine) and natural organic matter (NOM; fulvic and humic acids), which may chemically, or physically sorb onto NP surface and modify Ag NPs surface properties and colloidal stability (Yang et al., 2014; Pokhrel et al., 2013). For example hydrosulfide groups in NOM can form strong covalent bonds with Ag NPs surface and replace the original surface coating such as polyvinylpyrrolidone (PVP) (Stewart et al., 2012; Mandal et al., 2001), and thus reduce PVP-Ag NPs stability by increasing ionic strength (Gondikas et al., 2012). Aggregation of NPs (e.g. Ag NPs and Au NPs) can lead to a reduction in NP toxicity (Römer et al., 2013; Truong et al., 2011).

Few studies have investigated the effect of cysteine on the stability of Ag NPs (Pokhrel et al., 2013) and their fate and transport in porous media (Yang et al., 2014), typically at high Ag NP concentrations (ca. >1 mg L^{-1}) (Sharma et al., 2014; Yang et al., 2014; Pokhrel et al., 2013), and observed slight aggregation of cit- and PVP-Ag NPs over a period of 48 h. However, there are currently no studies on the impact of cystine on the behavior of Ag NPs, in particular at low NP concentrations.

The aim of this study is therefore to investigate the stability of citrate-, PVP- and PEG-coated Ag NPs following their interaction with cystine. In particular, we investigated the impact of cystine on cit-Ag NP aggregation kinetics at environmentally and eco-toxicologically relevant Ag NP concentrations (125–1000 μg L^{-1}), and the impact of SRFA on the interaction between cit-Ag NPs and cystine. We also investigated the aggregation of citrate, PVP and PEG-Ag NPs up to 24 h post interaction with different concentrations of cystine. Cystine (disulfide form of cysteine) and Suwannee River fulvic acid (SRFA) were chosen to represent two distinct types of NOM. Cystine and cysteine represent a class of small molecular weight metal-complexing ligands with a thiol and disulfide groups and are commonly present in surface waters at low concentrations (nM to μM range) (Gondikas et al., 2012; Ciglenecki et al., 2000). Cysteine is also widely used in Ag NP toxicity experiments to differentiate the toxicity of NP vs. Ag^+ ions. Cystine rather than cysteine was used in this study for the following reasons 1) the weaker affinity of the disulfide group to Ag^+, thus minimizing the impact on Ag NP dissolution and enabling the use of UV–vis to study the aggregation behavior of Ag NPs, 2) cysteine is highly reactive and readily oxidizes to cystine under oxic conditions (Van Vranken and Weiss, 2012; McBean, 2012), and 3) Cystine is the predominant form of in plasma, extracellular body fluids and cell culture media (Banjac et al., 2008). SRFA represent a class of less-defined natural macromolecules, which usually stabilize NPs (Baalousha, 2009; Baalousha et al., 2013).

2. Materials and methods

2.1. Chemicals

Silver nitrate (ACS grade, 99.9$^+$%) and sodium borahydrate (98%) were purchased from Alfa Aesar (Ward Hill, MA, USA). Trisodium citrate (Lab grade) was purchased from Fisher Scientific (Pittsburgh, PA, USA). Cystine (L-cystine ≥98% TLC) was purchased from Sigma Aldrich (St Louis, MO, USA). SRFA was purchased from the International Humic Substances Society (St Paul, MN, USA). All chemicals were used without further purification.

2.2. Synthesis and characterization of silver nanoparticles

Citrate-coated silver NPs (cit-Ag NPs) were synthesized and characterized as described in previous publications (Römer et al., 2011; Baalousha and Lead, 2012). Briefly, cit-Ag NPs (cit-Ag NPs) were prepared by the reduction of silver nitrate in trisodium citrate. A 100 mL of 0.31 mM trisodium citrate, 100 mL of 0.25 mM silver nitrate and 10 mM of sodium borohydride solutions were prepared in high purity water and kept at 4 °C in the dark for 30 min. The silver nitrate and trisodium citrate solutions were mixed together in a conical flask and vigorously stirred. Subsequently, 6 mL of the reducing agent, sodium borohydride ($NaBH_4$), was added in one batch. After 10 min of stirring, the solution was heated slowly to boiling and heated for a further 90 min, left overnight and cooled (4 °C, in the dark). Ag NPs were then cleaned, to remove the excess reagents before use, by ultrafiltration (Amicon, 1 kDa regenerated cellulose membrane, Millipore) using a diafiltration method to prevent NP aggregation and drying. Ag NPs were re-dispersed in 0.31 mM trisodium citrate solution to avoid further growth; this process was repeated at least three times. The concentration of Ag NPs was measured by inductively coupled plasma-optical emission spectroscopy and was about 10.0 ± 0.3 mg L^{-1}.

PVP- and PEG-Ag NPs were prepared by ligand exchange approach using citrate-coated Ag NPs as precursor as described elsewhere (Tejamaya et al., 2012). Aliquots of cit-Ag NPs were converted into PEG- and PVP-stabilized Ag NPs by adding 8 molecules of PVP, or 4 molecules of PEG per nm^2 surface area of Cit-Ag NPs under vigorous stirring (e.g. 700 rpm) for at least 1 h and then cooled overnight at 4 °C.

The size and electrophoretic mobility (EPM) was measured by dynamic light scattering and laser Doppler electrophoresis, respectively using a Malvern Zetasizer NanoZS Instrument (Malvern, USA). The Malvern Zeta potential transfer standard consisting of Latex dispersed in pH 9.2 buffer and has an EPM value of −42 mV (DTS1235, Malvern Instrument Limited) was used to verify the performance of the instrument and the zeta potential cell throughout the experiments.

The optical absorbance spectrum of Ag NPs were collected by a UV–vis spectrometer (UV-2600 Shimadzu, Santa Clara, CA, USA) using a 100 mm path length cuvette, which allowed analysis of Ag NPs at relatively low concentrations (125 to 1000 μg L^{-1}). UV–vis spectra of cit-Ag NPs suspensions were collected over wavelengths (λ) 200–900 nm.

2.3. Solution chemistry

The aggregation behavior of cit-Ag NPs was investigated by UV–vis spectroscopy in suspensions containing variable concentration of Ag NPs (125 to 1000 μg L^{-1}; 1.16–9.27 μM Ag) and cystine (0 to 72 mg L^{-1}; 0–300 μM), in the presence and absence of Suwannee River Fulvic acid (SRFA, 1 mg L^{-1}). No buffer was used to avoid interferences from ions in the buffer solution. For instance, phosphate anions (a component of the commonly used phosphate buffers) have been shown to induce the aggregation of hematite particles (Chorover et al., 1997) and titanium dioxide NPs (Domingos et al., 2010). The pH was measured throughout the experiment and was in the range 5.5–5.7.

A stock suspension of SRFA was prepared by dissolving 2 mg in 10 mL ultrahigh purity water (UHPW), and the pH was adjusted by adding aliquots NaOH to pH 7.0. The suspension was then filtered (450 nm) to remove any aggregated SRFA molecules. A stock suspension of 333 μM (80 mg L^{-1}) cystine was prepared by dissolving 8 mg of cystine in 100 mL of UHPW. The cystine stock suspension was prepared daily before performing the aggregation experiments to avoid losses of cystine by degradation (Gondikas et al., 2012).

For all experiments performed in the absence of SRFA, an aliquot (125, 250, 500, and 1000 μL) of Ag NPs stock suspension was diluted in UHPW and mixed with different aliquots of cystine to achieve a final volume of 10 mL, and thus NP concentrations of 125, 250, 500 and 1000 μg L^{-1}. For all experiments performed in the presence of SRFA, an aliquot of 2 and 4 mL of Ag NPs stock suspension was mixed with 0.8 and 0.4 mL of SRFA stock suspension and topped with UHPW to achieve a final volume of 8 mL, which resulted in a mixture of 20 and 10 mg L^{-1} SRFA and concentrations of Ag NPs of 2.5 and 5.0 mg L^{-1}. The mixtures were then left for 24 h to reach equilibrium before performing any aggregation kinetic experiments. Then 0.5 and 1 mL of the mixtures were mixed with cystine and topped with UHPW to 10 mL to achieve a final concentration of Ag NPs of 125 and 500 μg L^{-1}, SRFA of 1 mg L^{-1}, and cystine (0–266 μM).

2.4. Aggregation kinetics

To quantitatively measure the aggregation kinetics of cit-Ag NPs by UV–vis, the concentration of individual cit-Ag NPs was monitored over time by performing a time scan of the UV–vis absorbance at λ = 394 nm, corresponding to the specific plasmon resonance peak for the individual Ag NPs (Fig. 1a). The changes in the UV–vis absorbance λ = 394 nm can be attributed to NP aggregation or dissolution (Baalousha et al., 2013; Baalousha et al., 2015b). Analysis of dissolved Ag concentration by ICP-MS following centrifugal ultrafiltration at 3 kD over 24 h, well beyond the time required to determine NP aggregation kinetics, demonstrated that the differences in cit-Ag NP dissolution in the presence or absence of cystine was not significant (Fig. S1). Therefore, the changes in the UV–vis absorbance λ = 394 nm can be attributed to aggregation of primary Ag NPs. The aggregation rate constant is proportional to rate of change of the UV–vis at λ = 394 nm ($da_{\lambda=394}/d_t$, a refers to UV–vis absorption, Eq. (1)) during the early stage aggregation (Baalousha et al., 2013; Moskovits and Vlc, 2005); that is slope of the loss in the UV–vis absorbance at λ = 394 within the first 30 s after mixing Ag NPs with cystine, which was determined by fitting a linear correlation function.

$$k = \frac{1}{oN}\frac{da_{\lambda=394}}{d_t} \quad (1)$$

where N is the initial particle concentration and o is the optical factor.

For colloidal systems, plots of the attachment efficiency (α = 1/W, determined according to Eq. (2), where W is the stability ratio) against electrolyte concentration at a given experimental conditions can be used to characterize NP aggregation kinetics and suspension stability.

$$\alpha = \frac{1}{W} = \frac{k_{slow}}{k_{fast}} \quad (2)$$

where k_{slow} and k_{fast} represent the aggregation rate constant under reaction (RLA) and diffusion (DLA) limited aggregation regimes. The RLA regime occurs at counter ion concentrations below the critical coagulation concentration (CCC), whereas the DLA occurs at counter ion concentrations above the CCC. The CCC is frequently used to measure the stability of NP suspensions since it quantifies the minimum concentration of the ion/molecule that is required to completely destabilize the NP suspension (Elimelech and O'Melia, 1990). The attachment efficiencies under RLA and DLA regimes were fitted by linear functions and their intersections yield the respective CCC. The aggregation behavior of cit-Ag NPs was also monitored qualitatively by collecting the UV–vis spectra of Ag NPs 10 min post interaction with different concentrations of cystine over wavelength range 300–900 nm.

The zeta potential of Ag NPs and Ag NPs mixed with cystine were measured by laser Doppler electrophoresis using the same Malvern instrument. The reported zeta potentials and standard deviations were determined from 10 replicates of 50–100 runs each. The performance of the zeta potential cells was verified by measuring the zeta potential of the Malvern Zeta potential transfer standard and the zeta potential cell was replaced when any deviation from the standard value was observed.

The aggregation behavior of cit-, PEG- and PVP-Ag NPs was also monitored qualitatively by collecting the UV–vis spectra of Ag NPs over wavelength range 300–900 nm at 0, 6 and 24 h post mixing with different concentrations of cystine.

3. Results and discussion

3.1. Properties of the synthesized Ag NPs

According to the cumulant analysis, the z-d_h and polydispersity index of cit-Ag NPs in stock suspension are 16.6 ± 0.2 nm, 0.2 ± 0.1, respectively. Those of PEG-Ag NPs were 19.4 ± 0.3, and 0.29 ± 0.003 and those of PVP-Ag NPs were 21.6 ± 0.3 nm and 0.27 ± 0.005. The zeta potential of cit-Ag NPs, PEG-Ag NPs and PVP-Ag NPs was −46.5 ± 4.5 mV, −28.5 ± 1.4 mV, and −23.6 ± 1.1 mV, respectively. These measurements suggest that cit-, PEG- and PVP-Ag NPs are all well dispersed. The UV–vis spectra of the cit-Ag NPs, PEG-Ag NPs and PVP-Ag NPs in UHPW water shows a single peak centered at 394 nm, 394 nm, and 395 nm, respectively. Full characterization of the synthesized cit-Ag NPs are provided elsewhere (Baalousha et al., 2013; Römer et al., 2011; Baalousha and Lead, 2012).

3.2. Cystine induced aggregation of cit-Ag NPs

The UV–vis spectra of cit-Ag NPs, after 10 min of mixing with different concentrations of cystine (Fig. 1a–d) show a broadening of the UV–vis absorbance peak (centered on 394 nm) of as-synthesized cit-Ag NPs at low cystine concentrations (ca. 20 μM). At higher concentrations of cystine (ca. 33–83 μM), the UV–vis spectra show the formation of a

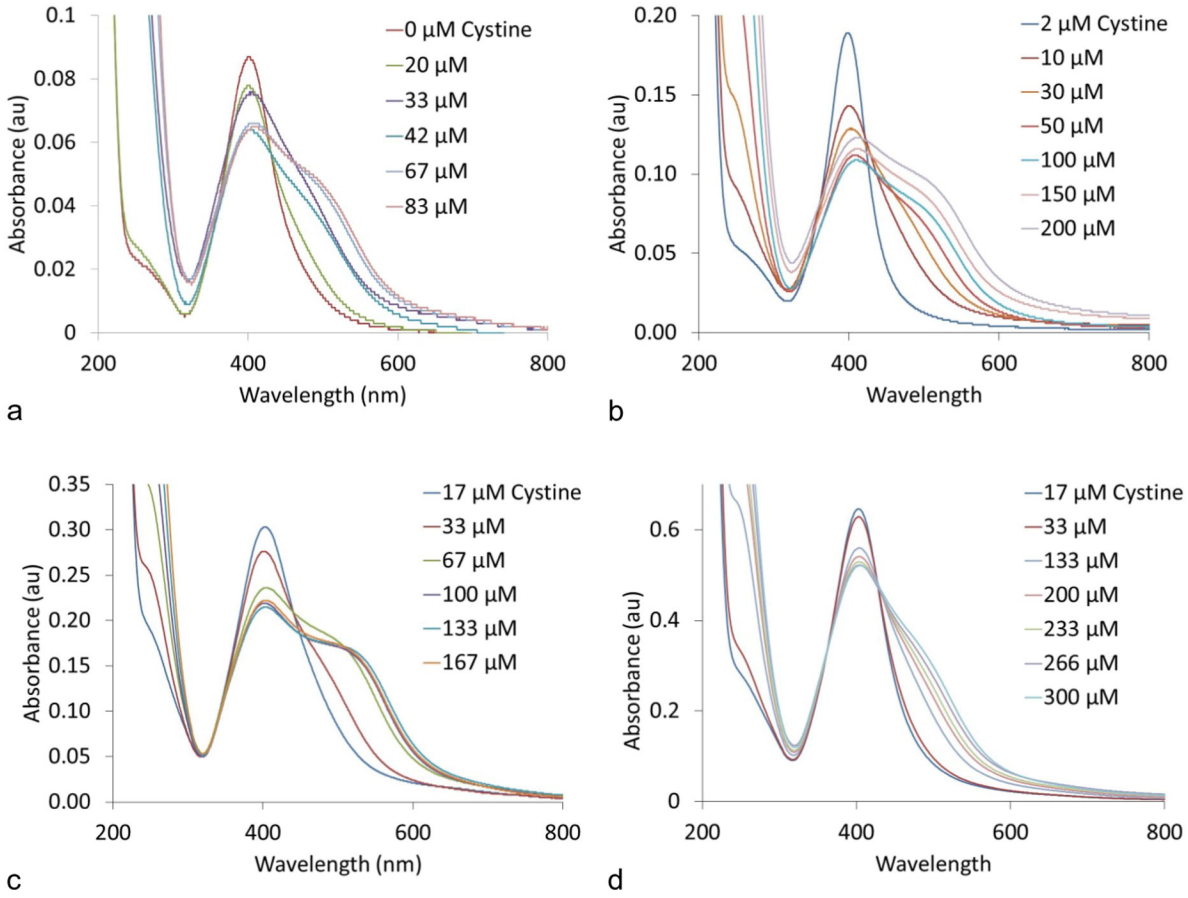

Fig. 1. UV–vis spectra of cit-Ag NP reacted with different concentrations of cystine at different concentrations of cit-AgNPs: (a) 125 μg L^{-1} Ag, (b) 250 μg L^{-1} Ag, (c) 500 μg L^{-1} Ag, and (d) 1000 μg L^{-1} Ag.

second peak centered on higher wavelengths in the visible and near infrared region (NIR) of the spectrum in the range of 500–650 nm. The increase in cystine concentration results in the decrease in the UV–vis absorbance at 394 nm and the increase of the second peak absorbance at 550–560 nm as a consequence of NP interactions, which indicates the loss of primary cit-Ag NPs by aggregation as observed elsewhere (Baalousha et al., 2013). Furthermore, at the same concentration of cystine (ca. 33 and 67 μM, Fig. S2), the second peak is shifted to higher wavelengths at lower NP concentrations compared to higher NP concentrations. The increased width of the second peak at lower NP concentrations is likely to be due to the formation of larger Ag NP aggregates (Baalousha et al., 2013), which can be attributed to the higher decrease in Ag NP surface charge with the decrease in cit-Ag NPs concentration (Fig. 2a) at the same concentration of cystine (discussed below). Under such conditions, more cystine molecules are available for interaction with the Ag surface atoms at lower Ag NP concentrations.

The UV absorbance at λ_{394} follows a first order decrease at low cystine concentrations and a more rapid, higher order decrease at high cystine concentrations (Fig. 2a–c). At the same concentration of cystine (Fig. S4), the relative loss in the UV–vis absorbance increase with the decrease in NP concentration, indicating higher removal of primary NPs by more aggregation at lower Ag NPs concentrations. The attachment efficiencies of cit-Ag NPs calculated from the loss of the UV–vis at λ_{394} are plotted in Fig. 3a, which generally shows RLA and DLA regimes and suggests that the aggregation kinetic of cit-Ag NPs in the presence of cystine are controlled by electrostatic interactions between the cystine coated AgNPs (see discussion below). The increased cystine concentration results in a decrease in the surface charge of the cit-Ag NPs (Fig. 2a). In the RLA regime, the cit-Ag NPs are kinetically stabilized by an electrostatic barrier resulting from the double layer repulsion and the van der Waals attractions forces. In the DLA, the surface charge of the cit-Ag NPs is sufficiently reduced by the cystine and the energy barrier is no longer sufficient to kinetically stabilize the particles, and therefore, aggregation process is only driven by diffusion. It was not possible to calculate the attachment efficiency at cit-Ag NP concentration of 1000 μg L^{-1} Ag as the concentration of cystine, within its limit of solubility, was not sufficient to induce DLA and thus it was not possible to calculate the fast aggregation rate.

At the same cystine concentration and under RLA regime (Fig. 3a), the attachment efficiency decreases with the increase in Ag NP concentration. This behavior can be attributed to the higher abundance of cystine per surface atom of Ag NPs at lower NP concentrations, resulting in higher coverage of the NP with cystine and therefore higher reduction in Ag NP surface charge. The CCC as a function of Ag NP concentration increases with the increase in NP concentration (Fig. 3b), which can be attributed again to the fact that cystine is more efficient in aggregating cit-Ag NPs at lower NP concentrations. This is the first time that cystine-induced concentration-dependent aggregation of cit-Ag NPs is demonstrated.

3.3. Effect of cystine on cit-Ag NPs surface charge

Cit-Ag NPs are negatively charged (zeta potential of -46.5 ± 4.5 mV). Fig. 2a shows the zeta potential of Ag NPs (125–1000 μg L^{-1}) as a function of cystine concentration, and shows that, for a fixed NP concentration, the magnitude of zeta potential decrease with the increase in cystine concentration. For a fixed cystine concentration, the magnitude of zeta potential decreases with the decrease in NP concentration. These observations are in agreement with the increased

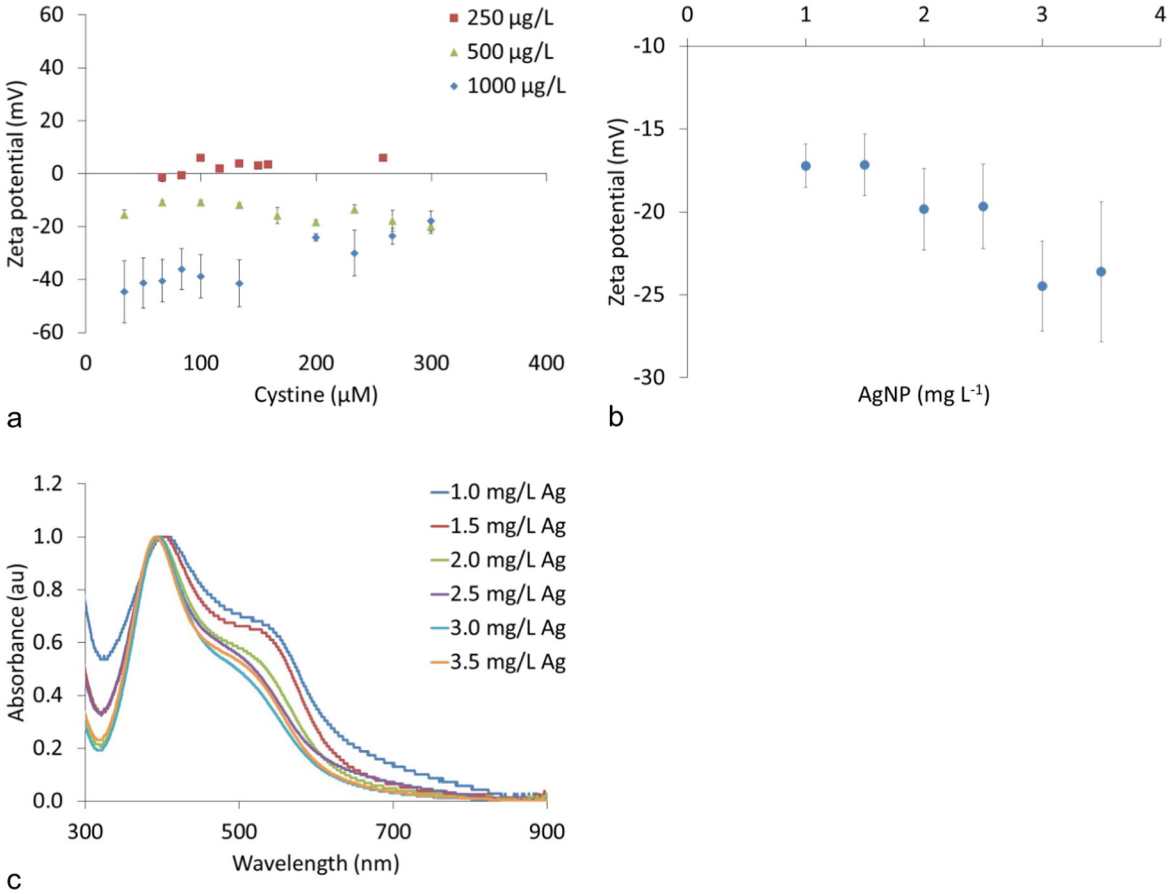

Fig. 2. Zeta potential of cit-Ag NPs reacted with cystine (a) at different concentrations of cystine and cit-Ag NPs, and (b) at fixed concentration of cystine (225 µM) and different concentrations of cit-Ag NPs (1–3.5 mg L^{-1}). (c) Uv–vis spectra of cit-Ag NPs 24 h post interaction with 225 µM cysteine.

aggregation of Ag NPs at higher cystine concentrations and lower NP concentrations.

High uncertainty was observed in the measured zeta potential at low NP concentrations as laser Doppler electrophoresis requires high NP concentrations, in the range of several mg L^{-1} (Malvern, 2005). Therefore, to further confirm the effect of cystine on the surface charge of cit-Ag NPs, a second set of experiments were performed at higher NP concentrations (1 to 3.5 mg L^{-1}) and at fixed cystine concentration (225 µM; Fig. 2b). Again, the results demonstrate that the magnitude of zeta potential of cit-Ag NPs decreased to lower values with the decrease in NP concentration (Fig. 2b). Thus, cystine is more efficient in reducing the surface charge of cit-Ag NPs at lower NP concentrations, which can be attributed to the higher cystine to surface Ag atom ratio at lower NP concentrations and thus the higher coverage of Ag NPs by cystine molecules.

The cystine-induced aggregation and surface charge alteration of cit-Ag NPs can be explained by the chemical interaction of the surface Ag atoms with the disulfide group in the cystine molecule and the zwitterion-type (Zwitterion is a neutral molecule with a positive and a negative electrical charge, though multiple positive and negative charges can be present) surface charge behavior of cystine molecules. It has been demonstrated that similar to the thiol group in cysteine, disulfide groups in cystine can sorb on the surface of AgNPs (Lopez-Tobar et al., 2013; Podstawka et al., 2004a). Additionally, Ag NPs have been

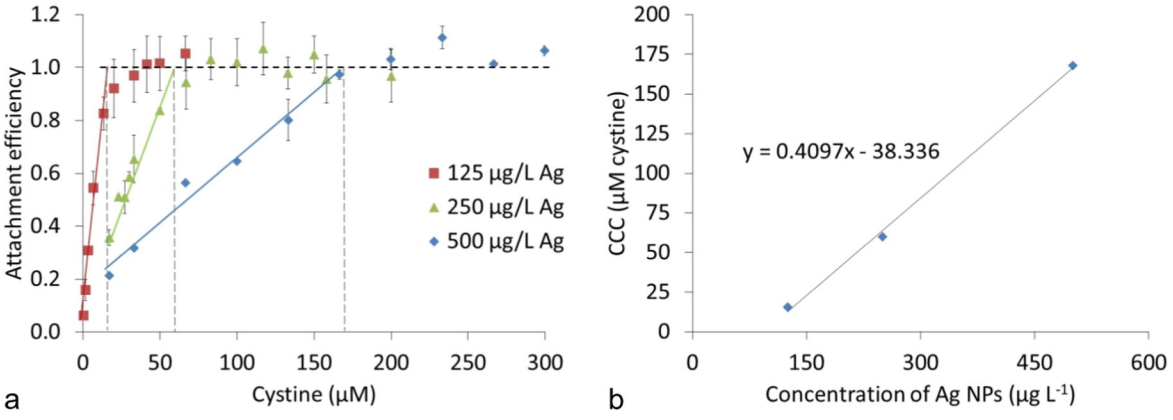

Fig. 3. Attachment efficiency of cit-Ag NPs reacted with cystine at different concentrations of cit-Ag NPs.

shown to induce S\S cleavage in cystine at low concentrations, but can keep intact S\S bonds bond at a concentration threshold of about 200 μM (Lopez-Tobar et al., 2013; Podstawka et al., 2004b; Lee et al., 1991), which may explain the similarity in the effect of cystine and cysteine in inducing the aggregation of silver NPs.

After cystine adsorption on the Ag NPs, the cystine molecule has still two functional groups (carboxylic and amine) to form bonds between particles. The pKa value of the carboxylic and amine groups are 1.96 and 8.18, respectively (Ravindran et al., 2012) and the isoelectric pH of cystine is 5.07. The pH of the Ag NPs-cystine mixture was about 5.5–5.7, thus cystine has a negative net charge at the experimental conditions. At this pH, the amine functional groups of cystine are protonated (positively charged, NH^{3+}), whereas the carboxylic groups are deprotonated (negatively charged, COO^{-}). Thus, the positively charged amino group in the cystine ($-NH^{3+}$) on the surface of one NP interacts with the negative charge on the surface of other Ag NP (carboxylic group, COO^{-}) through electrostatic attraction (Horovitz et al., 2007; Brewer et al., 2005), and cause aggregation (Ravindran et al., 2012). Hence, the cystine molecule constitutes a bridge among Ag NPs, thus inducing Ag NPs aggregation.

The concentration-dependent aggregation of Ag NPs in the presence of cystine is due to the ratio between Ag and cystine, and thus the surface coverage of Ag NPs by cystine. At lower Ag NP concentration, more cystine molecules are available to react with the surface of Ag NPs, resulting in a higher surface coverage of Ag NPs by cystine, reduction of surface charge of Ag NPs, and increased aggregation of Ag NPs. This is further supported by the shift to higher wavelengths (approximately 10 nm) in the Plasmon resonance of Ag NPs at lower NP concentrations in the presence of cystine (Fig. 2c), indicating increased interaction with cystine at low NP concentrations.

3.4. Aggregation impacted by fulvic acid

The UV–vis spectra of cit-Ag NPs 10 min post interaction with cystine in the presence of SRFA show little to no change in the spectra in term of peak broadening or absorbance loss at 394 nm (Fig. S5a and b), suggesting that SRFA prevents (or reduce) cystine induced aggregation of cit-Ag NPs. The rate of the decay λ_{394} is generally slower and decays to higher absorbance in the presence of SRFA (~0.88, Fig. S5a and b) compared to the absence of SRFA (~0.6, Fig. 2a and c), presumably due to the reduced aggregation of cit-Ag NPs in the presence of SRFA. It was not possible to calculate the attachment efficiency in the presence of SRFA because aggregation of cit-Ag NPs did not reach the fast aggregation regime (DLA) within the limit of cystine solubility in water (333 μM). Nonetheless, the rate loss of UV–vis_{394} increases slightly with the increase in cystine concentration, but does not reach the fast aggregation rate (Fig. 4a).

It is well known that SRFA forms a surface coating on cit-Ag NPs and increase the surface charge and provide steric stabilization (Baalousha, 2009; Diegoli et al., 2008; Tipping and Higgins, 1982; Baalousha et al., 2008) to cit-Ag NPs. Therefore, the sorption of SRFA molecules on cit-Ag NPs increases electrosteric stabilization of cit-Ag NPs, but they do not completely inhibit surface charge screening and NP aggregation by electrolytes (Baalousha et al., 2013; Chen and Elimelech, 2007). It is worth noting that, in the presence of SRFA, the surface charge of cit-Ag NPs did not change with the increase in cystine concentrations

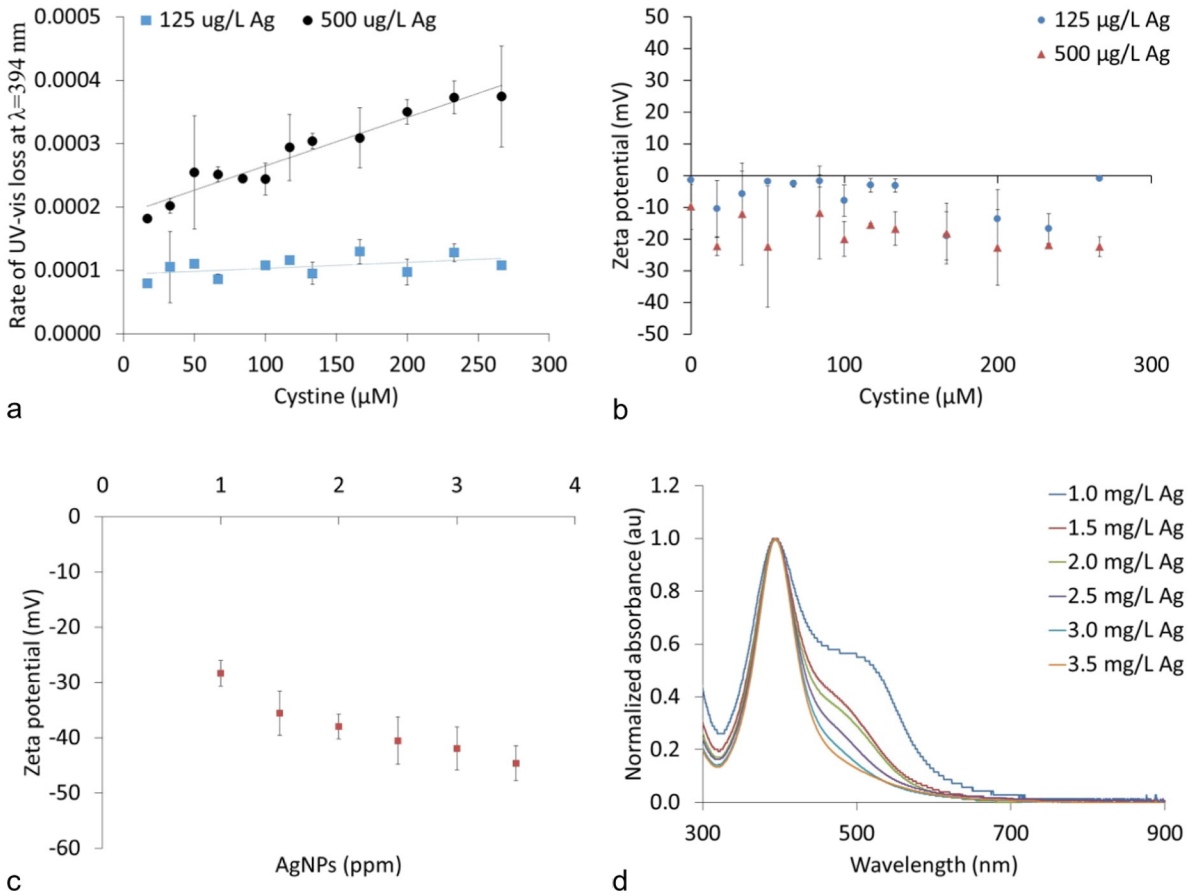

Fig. 4. (a) Rate loss of the UV–vis absorbance at 394 nm as a function of cystine concentration in the presence of 1 mgL^{-1} SRFA, (b) zeta potential of cit-Ag NPs reacted with cystine in the presence of 1 mgL^{-1} SRFA, and (c) zeta potential of cit-Ag NPs reacted with fixed concentration of cystine (225 μM) and different concentrations of cit-Ag NPs (1–3.5 mg L^{-1}). (d) Normalized Uv–vis spectra of cit-AgNPs 24 post reaction with cystine.

(Fig. 4b), which can be attributed to the lack of interaction between cystine and the surface of Ag NPs. Similarly to the case of without SRFA, another set of experiment was conducted to measure the zeta potential of Ag NPs 24 h post interaction with cystine in the presence of SRFA at higher Ag NP concentrations (1.0–3.5 mg L^{-1} Ag) to avoid any uncertainty in the measured zeta potential at low NP concentrations (Fig. 4c). The results suggest that the magnitude of the zeta potential decreases with the decrease in NP concentration at constant cystine concentration (225 μM), indicating the increased efficiency of surface charge alteration at lower NP concentrations due to the increased probability of surface Ag atoms-cystine interactions. Nonetheless, the magnitude of the zeta potential in the presence of SRFA (ca. −28 to −44 mV) remains higher compared with that in the absence of SRFA (ca. −17 to −24 mV), indicating that SRFA form a surface coating on Ag NPs, enhance their surface charge and thus their stability in the presence of cystine. The UV–vis of Ag NPs spectra 24 h post interaction with cystine in the presence of SRFA shows no shift in the first peak position with the change in NP concentrations (Fig. 4d) confirming that SRFA limits the interaction of cystine with surface of Ag NPs. Furthermore, Fig. 4d shows the formation of a second peak at higher wavelengths. For the same concentration of Ag NPs, the absorbance of the second peak is lower in the presence of SRFA (Fig. 4d) compared with that in the absence of SRFA (Fig. 2c), again confirming the role of SRFA in reducing the cystine-induced aggregation of Ag NPs.

3.5. Aggregation impacted by NP surface coating

It is well known that surface coatings have a significant impact on NP stability and aggregation. Whereas citrate and PEG stabilize Ag NPs via electrostatic repulsion, PVP stabilizes Ag NPs via steric stabilization mechanism (Baalousha et al., 2013; Tejamaya et al., 2012). Therefore, citrate and PEG coated Ag NPs are susceptible to aggregation by charge screening by electrolytes, whereas PVP coated Ag NPs are generally stable at a wide range of ionic strengths and pHs (Baalousha et al., 2013; Tejamaya et al., 2012). Here, we investigate the impact of cystine on the stability of PEG- and PVP-Ag NPs at ecotoxicologically relevant and near environmentally relevant Ag NP concentrations.

The UV–vis absorbance of Cit-, PEG- and PVP-coated Ag NPs (225 μg L^{-1}) immediately after addition of different concentrations of cystine (7–133 μ) are presented in Fig. 5a, d and f, together with those after 6 h (Fig. 5b, e and h) and 24 h (Fig. 5c, f and i). All spectra show two peaks, the first centered on 394 to 402 nm, 393–400 nm and 393–412.5 nm immediately after addition of cystine for citrate-, PVP- and PEG coated Ag NPs, respectively. The position of the first peak shifts

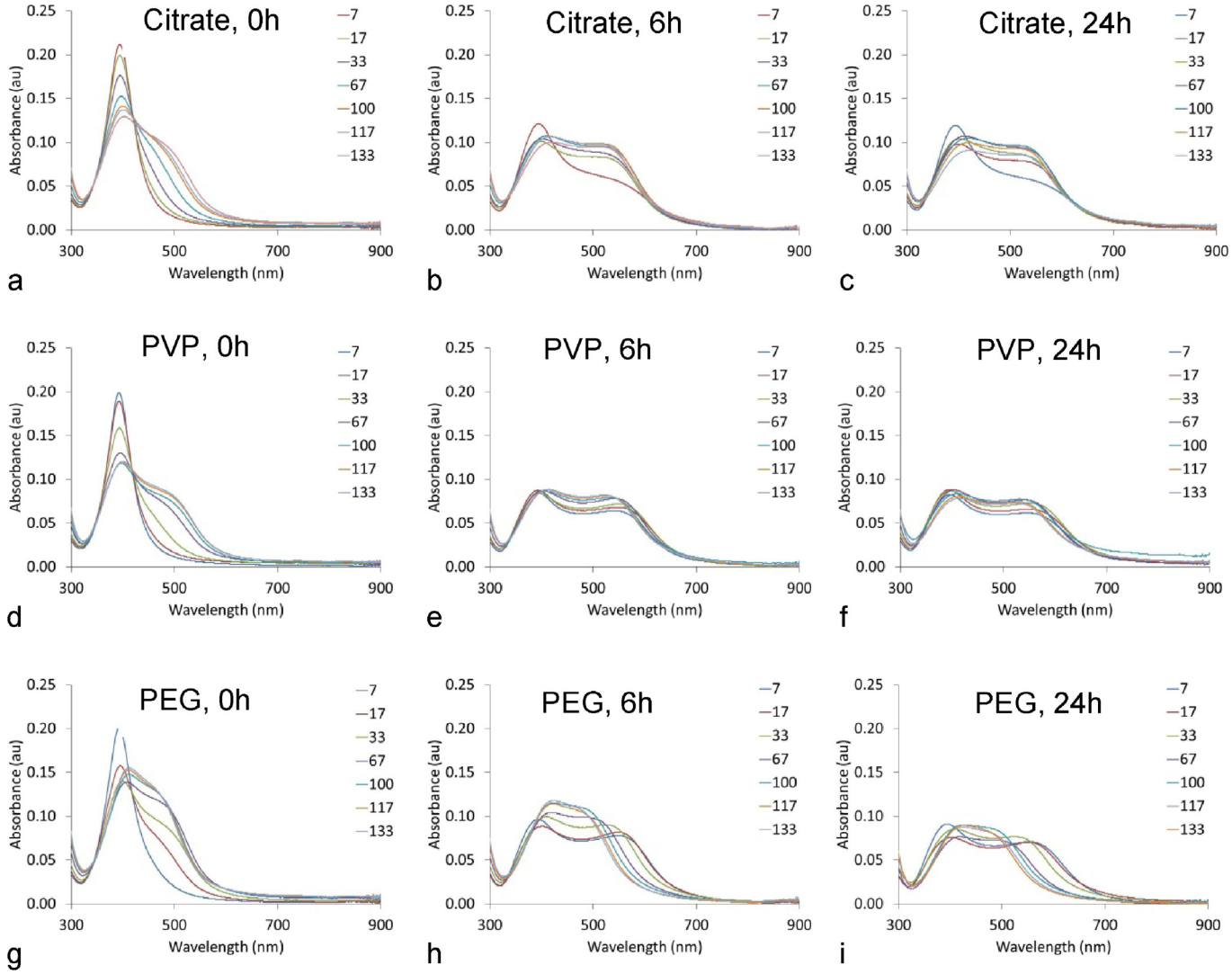

Fig. 5. UV–vis spectra of AgNPs (225 μg L^{-1}) with different surface coatings (a–c) citrate, (d–f) PVP, and (g–i) PEG at different time points (a, d, g) 0, (b, e, h) 6 and (c, f, i) 24 h following reaction with different concentrations of cystine (7–133 μM).

to higher wavelengths at higher concentrations of cystine indicating increased interaction between Ag NP surface atoms and cystine molecules. These observations confirm that cystine replaces the three types of surface coatings (citrate, PVP and PEG). The higher shift at higher cystine concentrations indicates increased interaction between Ag NP surface atoms and cystine molecules.

The first peak shifts to higher wavelength with time; ca. 394–422 nm, 394–415 nm, and 393–424 nm, for citrate-, PVP, and PEG coated Ag NPs 6 h post interactions with cystine. The position of this peak remains constant beyond 6 h up to 24 h, indicating that cystine-Ag NP surface atom interaction reaches equilibrium within 6 h.

The second peak is centered on 495 nm immediately after addition of cystine, shifts to higher wavelengths (ca. 530 nm) between 0 and 6 h and remains constant afterwards. These results indicate that cystine induces the aggregation of citrate, PEG and PVP coated Ag NPs, and that under the selected experimental conditions, Ag NPs occur both as primary Ag NPs as well as aggregated Ag NPs. These findings suggest that cystine binds to the surface of Ag NPs and replaces PVP and PEG coating similar to citrate, resulting in modification of NP surface coating and charge and therefore their aggregation behavior, in good agreement with other studies (Yang et al., 2014). The Plasmon resonance peaks was stable within 6 h indicating that Ag NPs were stable at this time point and did not undergo any further aggregation. No losses in the Plasmon resonance were observed at 24 h compared to 6 h indicating that aggregation resulted in the formation of small Ag NP aggregates that did not settle out of suspension. These findings are in good agreement with previous results suggesting that cystine induces aggregation of PVP-coated Ag NPs (Yang et al., 2014; Gondikas et al., 2012).

3.6. Environmental and nanotoxicological implications

This research represents the first systematic study of the effect of cystine concentration on the aggregation of Ag NPs at ecotoxicologically relevant and near environmentally relevant Ag NP concentrations. Cystine significantly impacts the stability of citrate, PEG and PVP coated Ag NPs, resulting in Ag NP aggregation in a concentration-dependent manner, with a shift in the CCC toward lower concentrations of cystine at lower concentration of Ag NPs. SRFA reduced the cystine induced aggregation of Ag NPs within the limit of cystine solubility in water, likely due to the steric effect of SRFA. Consequently, in natural surface waters, it is likely that cystine will play an important role in determining the fate and behavior of cit-Ag NPs, and further research is required to investigate the interplay between cystine, electrolytes and NOM on the stability of Ag NPs. Due to the higher affinity of the cysteine thiol groups to Ag^+ and Ag surfaces compared with the cystine disulfide group, a similar concentration-dependent aggregation of Ag NPs in the presence of cysteine is expected. Several studies have demonstrated that cysteine induces aggregation of Ag NPs (Gondikas et al., 2012), but none has investigated the concentration-dependent aggregation of Ag NPs in the presence of cysteine.

In ecotoxicological studies of Ag NPs, cysteine is typically used to scavenge the dissolved ions and thus to differentiate dissolved vs. NP effects assuming no interaction occurs between Ag NPs and cysteine. Several papers have reported lower toxicity of Ag NPs in the presence of cysteine, and consequently concluded that silver ions are the major cause of their antimicrobial activity. Our results suggest that the reduced toxicity in the presence of cysteine widely observed in the literature could be due to a combined effect of Ag^+ scavenging by cysteine and Ag NP aggregation. The concentration-dependent aggregation of Ag NPs induced by cystine (a similar behavior is expected with cysteine) can alter the nature of the dose (toxicant) in a typical dose-response experiment; that is Ag NPs may form aggregates at low concentration and stay suspended as individual NPs at high Ag NP concentration.

This work underscores the importance of understanding the impact of biogeochemical molecules on NP stability in both ecotoxicological media as well as in the natural environment, and thus the fate and effects of NPs. This study also underscores the importance of investigating NP interactions at environmentally and toxicologically relevant NP concentrations.

Acknowledgment

We acknowledge funding from the National Science Foundation (NSF1437307), funding from the SmartState Center for Environmental Nanoscience and Risk (CENR), along with the Morris College and department of energy-environmental management (DOE-EM) summer research experience program.

Appendix A. Supplementary data

Supplementary data to this article can be found online at http://dx.doi.org/10.1016/j.scitotenv.2016.02.212.

References

Baalousha, M., 2009. Aggregation and disaggregation of iron oxide nanoparticles: influence of particle concentration, PH and natural organic matter. Sci. Total Environ. 407 (6), 2093–2101.
Baalousha, M., Lead, J.R., 2012. Rationalizing nanomaterial sizes measured by atomic force microscopy, flow field-flow fractionation, and dynamic light scattering: sample preparation, polydispersity, and particle structure. Environ. Sci. Technol. 46 (11), 6134–6142.
Baalousha, M., Manciulea, A., Cumberland, S., Kendall, K., Lead, J.R., 2008. Aggregation and surface properties of iron oxide nanoparticles; influence of PH and natural organic matter. Environ. Toxicol. Chem. 27 (9), 1875–1882.
Baalousha, M., Nur, Y., Römer, I., Tejamaya, M., Lead, J.R., 2013. Effect of monovalent and divalent cations, anions and fulvic acid on aggregation of citrate-coated silver nanoparticles. Sci. Total Environ. 454–455 (0), 119–131.
Baalousha, M., Sikder, M., Prasad, A., Lead, J., Merrifield, R., Chandler, G.T., 2015a. The concentration-dependent behavior of nanoparticles. Environ. Chem. http://dx.doi.org/10.1071/EN15142.
Baalousha, M., Arkill, K.P., Romer, I., Palmer, R.E., Lead, J.R., 2015b. Transformations of citrate and tween coated silver nanoparticles reacted with Na2S. Sci. Total Environ. 502 (0), 344–353.
Banjac, A., Perisic, T., Sato, H., Seiler, A., Bannai, S., Weiss, N., Kölle, P., Tschoep, K., Issels, R.D., Daniel, P.T., 2008. The cystine/cysteine cycle: a redox cycle regulating susceptibility versus resistance to cell death. Oncogene 27 (11), 1618–1628.
Benn, T.M., Westerhoff, P., 2008. Nanoparticle silver released into water from commercially available sock fabrics. Environ. Sci. Technol. 42 (11), 4133–4139.
Brewer, S.H., Glomm, W.R., Johnson, M.C., Knag, M.K., Franzen, S., 2005. Probing BSA binding to citrate-coated gold nanoparticles and surfaces. Langmuir 21 (20), 9303–9307.
Chen, K.L., Elimelech, M., 2007. Influence of humic acid on the aggregation kinetics of fullerene (C60) nanoparticles in monovalent and divalent electrolyte solutions. J. Colloid Interface Sci. 309 (1), 126–134.
Chorover, J., Zhang, J., Amistadi, M.K., Buffle, J., 1997. Comparison of hematite coagulation by charge screening and phosphate adsorption; differences in aggregate structure. Clay Clay Miner. 45 (5), 690–708.
Ciglenecki, I., Cosovic, B., Vojvodic, V., Plavsic, M., Furic, K., Minacci, A., Baldi, F., 2000. The role of reduced sulfur species in the coalescence of polysaccharides in the Adriatic Sea. Mar. Chem. 71 (3–4), 233–249.
Diegoli, S., Manciulea, A.L., Begum, S., Jones, I.P., Lead, J.R., Preece, J.A., 2008. Interaction between manufactured gold nanoparticles and naturally occurring organic macromolecules. Sci. Total Environ. 402 (1), 51–61.
Domingos, R.F., Peyrot, C., Wilkinson, K.J., 2010. Aggregation of titanium dioxide nanoparticles: role of calcium and phosphate. Environ. Chem. 7 (1), 61–66.
El Badawy, A.M., Silva, R.G., Morris, B., Scheckel, K.G., Suidan, M.T., Tolaymat, T.M., 2011. Surface charge-dependent toxicity of silver nanoparticles. Environ. Sci. Technol. 45 (1), 283–287.
Elimelech, M., O'Melia, C.R., 1990. Kinetics of deposition of colloidal particles in porous media. Environ. Sci. Technol. 24 (10), 1528–1536.
George, S., Lin, S., Ji, Z., Thomas, C., Li, L., Mecklenburg, M., Meng, H., Wang, X., Zhang, H., Xia, T., Hohman, J.N., Lin, S., Zink, J.I., Weiss, P.S., Nel, A.E., 2012. Surface defects on plate-shaped silver nanoparticles contribute to its hazard potential in a fish gill cell line and zebrafish embryos. ACS Nano 6 (5), 3745–3759.
Gondikas, A.P., Morris, A., Reinsch, B.C., Marinakos, S.M., Lowry, G.V., Hsu-Kim, H., 2012. Cysteine-induced modifications of zero-valent silver nanomaterials: implications for particle surface chemistry, aggregation, dissolution, and silver speciation. Environ. Sci. Technol. 46 (13), 7037–7045.
Horovitz, O., Tomoaia, G., Mocanu, A., Yupsanis, T., Tomoaia-Cotisel, M., 2007. Protein binding to gold colloids. Gold Bull. 40 (3), 213–218.
Jin, X., Li, M., Wang, J., Marambio-Jones, C., Peng, F., Huang, X., Damoiseaux, R., Hoek, E.M.V., 2010. High-throughput screening of silver nanoparticle stability and bacterial inactivation in aquatic media: influence of specific ions. Environ. Sci. Technol. 44 (19), 7321–7328.
Kaegi, R., Sinnet, B., Zuleeg, S., Hagendorfer, H., Mueller, E., Vonbank, R., Boller, M., Burkhardt, M., 2010. Release of silver nanoparticles from outdoor facades. Environ. Pollut. 158 (9), 2900–2905.

Kawata, K., Osawa, M., Okabe, S., 2009. In vitro toxicity of silver nanoparticles at noncytotoxic doses to HepG2 human hepatoma cells. Environ. Sci. Technol. 43 (15), 6046–6051.
Lee, H., Kim, M.S., Suh, S.W., 1991. Raman spectroscopy of sulphur-containing amino acids and their derivatives adsorbed on silver. J. Raman Spectrosc. 22 (2), 91–96.
Lopez-Tobar, E., Hernández, B., Ghomi, M., Sanchez-Cortes, S., 2013. Stability of the disulfide bond in cystine adsorbed on silver and gold nanoparticles as evidenced by SERS data. J. Phys. Chem. C 117 (3), 1531–1537.
Lubick, N., 2008. Nanosilver toxicity: ions, nanoparticles or both? Environ. Sci. Technol. 42 (23), 8617.
Malvern, 2005. Concentration Limits for Zeta Potential Measurements in the Zetasizer Nano.
Mandal, S., Gole, A., Lala, N., Gonnade, R., Ganvir, V., Sastry, M., 2001. Studies on the reversible aggregation of cysteine-capped colloidal silver particles interconnected via hydrogen bonds. Langmuir 17 (20), 6262–6268.
McBean, G.J., 2012. Astrocytes and the regulation of cerebral cysteine/cystine redox potential: implications for cysteine neurotoxicity. In: Chorkina, F.V., Karataev, A.I. (Eds.), Cysteine: Biosynthesis, Chemical Structure and Toxicity. Nova Science Publishers, Hauppauge,NY.
Miao, A.-J., Luo, Z., Chen, C.-S., Chin, W.-C., Santschi, P.H., Quigg, A., 2011. Intracellular uptake: a possible mechanism for silver engineered nanoparticle toxicity to a freshwater alga *Ochromonas danica*. PLoS ONE 5 (12) e15196-1–e15196-8.
Mirshahghassemi, S., Lead, J.R., 2015. Oil recovery from water under environmentally relevant conditions using magnetic nanoparticles. Environ. Sci. Technol. 49 (19), 11729–11736.
Moskovits, M., Vlc ková, B., 2005. Adsorbate-induced silver nanoparticle aggregation kinetics. J. Phys. Chem. B. 109 (31), 14755–14758.
Navarro, E., Piccapietra, F., Wagner, B., Marconi, F., Kaegi, R., Odzak, N., Sigg, L., Behra, R., 2008. Toxicity of silver nanoparticles to *Chlamydomonas reinhardtii*. Environ. Sci. Technol. 42 (23), 8959–8964.
NNI, 2014. National Nanotechnology Initiative.
Podstawka, E., Ozaki, Y., Proniewicz, L.M., 2004a. Adsorption of S-S containing proteins on a colloidal silver surface studied by surface-enhanced raman spectroscopy. Appl. Spectrosc. 58 (10), 1147–1156.
Podstawka, E., Ozaki, Y., Proniewicz, L.M., 2004b. Part I: surface-enhanced Raman spectroscopy investigation of amino acids and their homodipeptides adsorbed on colloidal silver. Appl. Spectrosc. 58 (5), 570–580.
Pokhrel, L.R., Dubey, B., Scheuerman, P.R., 2013. Impacts of select organic ligands on the colloidal stability, dissolution dynamics, and toxicity of silver nanoparticles. Environ. Sci. Technol. 47 (22), 12877–12885.
Pokhrel, L.R., Dubey, B., Scheuerman, P.R., 2014. Natural water chemistry (dissolved organic carbon, PH, and hardness) modulates colloidal stability, dissolution, and antimicrobial activity of citrate functionalized silver nanoparticles. Environ. Sci.: Nano. 1 (1), 45–54.
Ravindran, A., Dhas, S.P., Chandrasekaran, N., Mukherjee, A., 2012. Differential interaction of silver nanoparticles with cysteine. J. Exp. Nanosci. 8 (4), 589–595.
Römer, I., White, T.A., Baalousha, M., Chipman, K., Viant, M.R., Lead, J.R., 2011. Aggregation and dispersion of silver nanoparticles in exposure media for aquatic toxicity tests. J. Chromatogr. A. 1218 (27), 4226–4233.
Römer, I., Gavin, A.J., White, T.A., Merrifield, R.C., Chipman, J.K., Viant, M.R., Lead, J.R., 2013. The critical importance of defined media conditions in *Daphnia magna* nanotoxicity studies. Toxicol. Lett. 0.
Royal Society & Royal Academy Engineering Nanoscience and Nanotechnologies, 2004a. Opportunities and Uncertainties.
Sharma, V.K., Siskova, K.M., Zboril, R., Gardea-Torresdey, J.L., 2014. Organic-coated silver nanoparticles in biological and environmental conditions: fate, stability and toxicity. Adv. Colloid Interf. Sci. 204 (0), 15–34.
Silva, T., Pokhrel, L.R., Dubey, B., Tolaymat, T.M., Maier, K.J., Liu, X., 2014. Particle size, surface charge and concentration dependent ecotoxicity of three organo-coated silver nanoparticles: comparison between general linear model-predicted and observed toxicity. Sci. Total Environ. 468–469 (0), 968–976.
Smetana, A.B., Klabunde, K.J., Marchin, G.R., Sorensen, C.M., 2008. Biocidal activity of nanocrystalline silver powders and particles. Langmuir 24 (14), 7457–7464.
Stewart, A., Zheng, S., McCourt, M.A.R., Bell, S.E.J., 2012. Controlling assembly of mixed thiol monolayers on silver nanoparticles to tune their surface properties. ACS Nano 6 (5), 3718–3726.
Tejamaya, M., Römer, I., Merrifield, R.C., Lead, J.R., 2012. Stability of citrate, PVP, and PEG coated silver nanoparticles in ecotoxicology media. Environ. Sci. Technol. 46 (13), 7011–7017.
Tipping, E., Higgins, D.C., 1982. The effect of adsorbed humic substances on the colloid stability of haematite particles. Colloids Surf. 5 (2), 85–92.
Truong, L., Zaikova, T., Richman, E.K., Hutchison, J.E., Tanguay, R.L., 2011. Media ionic strength impacts embryonic responses to engineered nanoparticle exposure. Nanotoxicology 6 (7), 691–699.
Van Vranken, D., Weiss, G., 2012. Introduction to Bioorganic Chemistry and Chemical Biology. Garland Science.
Woodrow Wilson data base, 2014. The Project on Emerging Nanotechnologies (http://www.nanotechproject.org/) .
Xiu, Z.M., Zhang, Q.B., Puppala, H.L., Colvin, V.L., Alvarez, P.J.J., 2012. Negligible particle-specific antibacterial activity of silver nanoparticles. Nano Lett. 12 (8), 4271–4275.
Yang, X., Lin, S., Wiesner, M.R., 2014. Influence of natural organic matter on transport and retention of polymer coated silver nanoparticles in porous media. J. Hazard. Mater. 264 (0), 161–168.